

Supplementary Materials

Synergetic effect of h-BN shells and subsurface B in CoBx@h-BN nanocatalysts for enhanced oxygen evolution reactions

Siru Chen,^a Yanqiang Li,^b Zhihua Zhang,^c Qiang Fu,^{*a} and Xinhe Bao^a

^a *State Key Laboratory of Catalysis, iChEM, Dalian Institute of Chemical Physics, the
Chinese Academy of Sciences, Dalian 116023, P.R. China*

^b *State Key Laboratory of Fine Chemicals, School of Petroleum and Chemical
Engineering, Dalian University of Technology, Panjin 124221, P. R. China*

^c *School of Materials Science and Engineering, Dalian Jiaotong University, Dalian
106028, P. R. China*

Email: qfu@dicp.ac.cn; Tel: 0086-411-84379253

Experimental Section

Synthesis of Co-B alloys. 50 mL of 2.0 M aqueous KBH_4 containing 0.20 M NaOH as the stabilizer was dropped slowly to 125 mL of 0.20 M CoCl_2 aqueous solution under the protection of Ar at 273 K. Black precipitates were separated from the solution with a magnet, and washed with deoxygenated distilled water until $\text{pH} = 7$ was reached. The powder was further washed with absolute ethanol. The Co-B amorphous alloys were treated in Ar at 250, 400, 550, 700, and 850 °C, respectively, for 2 h. The materials were labeled as $\text{CoB}_x\text{-T}$ (T represents the annealing temperature).

Synthesis of $\text{CoB}_x@h\text{-BN}$ catalysts. Co-B amorphous alloy was loaded into a fixed-bed micro-reactor and purged with Ar ($70 \text{ mL}\cdot\text{min}^{-1}$) for 30 min to remove oxygen and moisture. The stream was then switched to NH_3 ($70 \text{ mL}\cdot\text{min}^{-1}$) and the sample was treated at the target temperature for 2 h. The treatment temperatures were chosen at 250, 400, 550, 700, and 850 °C, respectively. The samples are labeled as $\text{CoB}_x@h\text{-BN-T}$, in which T represents the treatment temperature.

Characterizations. Powder X-ray diffraction experiments were collected on an Empyrean diffractometer using a Cu $\text{K}\alpha$ ($\lambda = 1.5406 \text{ \AA}$) radiation source and a scanning rate of $12 \text{ }^\circ\text{C}\cdot\text{min}^{-1}$. X-ray photoelectron spectroscopy was performed in a Thermo Scientific ESCALAB 250Xi spectrometer using an Al $\text{K}\alpha$ X-ray source and pass energy of 20 eV. The binding energies were calibrated internally by C 1s binding energy (BE) at 284.5 eV from contamination carbon. Transmission electron microscopy (TEM) was carried out on a Hitachi HT 7700 microscope operated at an acceleration voltage of 100 kV, and high-resolution transmission electron microscopy (HRTEM) was recorded on an FET Tecnai F30 microscope at an accelerating voltage of 300 kV. The samples were ultrasonically dispersed in ethanol and placed onto a carbon film supported on a copper grid. Electron energy loss spectroscopy (EELS) was carried on a JEOL JEM-2100F microscope operated at 200 kV. High-sensitivity

low-energy ions scattering (HS-LEIS) analysis was carried out on an Ion-TOF Qtac100 low energy ion scattering analyzer. The actual concentrations of Co and B in all catalysts were determined by inductively coupled plasma optical emission spectroscopy (ICP-OES; Optima 7300DV, PerkinElmer). Nitrogen adsorption/desorption measurements were carried out at -196 °C with Autosorb iQ MP (Quantachrome Instruments) to determine surface area. Before sorption analysis, the samples were outgassed at 200 °C for 1 h before each measurement. Specific surface areas were calculated from nitrogen adsorption data by multipoint Brunauer-Emmett-Teller (BET) analysis. Fourier transform infrared (FTIR) spectra (KBr, Aldrich) were measured using a Thermo-Fisher scientific Nicolet iS50 FT-IR instrument. Samples were packed firmly to obtain transparent films.

Electrochemical measurements. Catalytic tests were performed in a standard three-electrode system with a rotating disk electrode (RDE) device from Pine Instrument Company connected to a CHI 660C potentiostat workstation. A glassy carbon disk (5 mm in diameter) was used as the working electrode, Ag/AgCl was used as the reference electrode, and a platinum wire was used as the counter electrode. The electrolyte is 1 M KOH solution. For preparation of the working electrode, 4 mg of the as-prepared catalyst was dispersed into a mixture of water (480 μ L) and isopropanol (480 μ L) solution and 20 μ L of Nafion solution (5 wt. %) was added, which was ultrasonically treated for 30 minutes to form a uniform catalyst ink. 8 μ L of catalyst ink was dipped onto the glass carbon electrode to get a loading amount of 0.167 mg cm⁻². RuO₂/C catalyst ink was prepared according to the same procedure. Before each test, the solution was bubbled with O₂ for 30 min to reach oxygen saturation. All potentials were measured against the reference electrode and converted to the reversible hydrogen electrode (RHE) reference scale by $E(\text{RHE}) = E(\text{Ag/AgCl}) + 0.059\text{pH} + 0.197$. The current densities in both CV and RDE data were normalized to the geometric area (0.196 cm²) of the glassy carbon electrode.

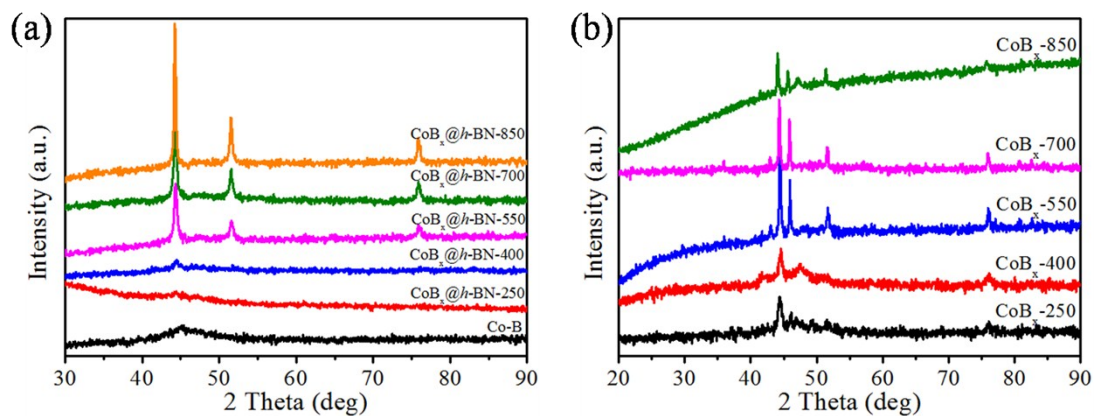


Figure S1 Powder XRD patterns of (a) Co-B and CoB_x@h-BN-T samples, and (b) CoB_x-T samples.

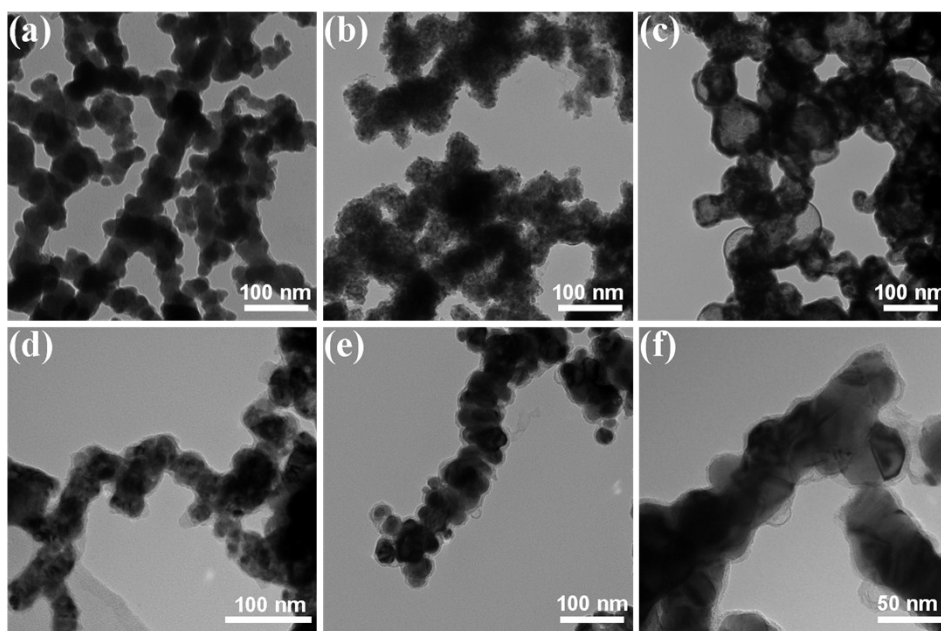


Figure S2 TEM images of Co-B amorphous alloy and CoB_x@h-BN-T samples: (a) Co-B, (b) CoB_x@h-BN-250, (c) CoB_x@h-BN-400, (d) CoB_x@h-BN-550, (e) CoB_x@h-BN-700, and (f) CoB_x@h-BN-850 samples.

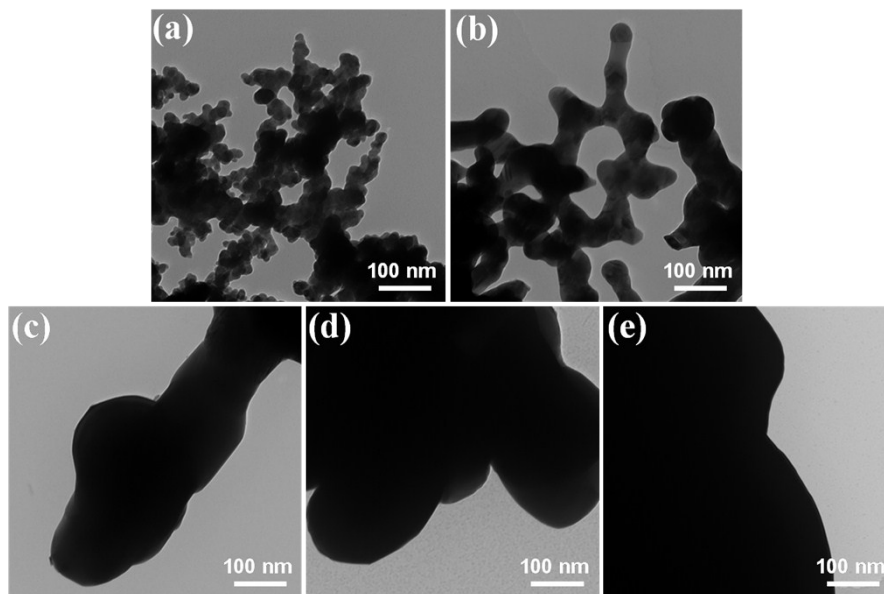


Figure S3 TEM images of $\text{CoB}_x\text{-T}$ samples: (a) $\text{CoB}_x\text{-250}$, (b) $\text{CoB}_x\text{-400}$, (c) $\text{CoB}_x\text{-550}$, (d) $\text{CoB}_x\text{-700}$, and (e) $\text{CoB}_x\text{-850}$ samples.

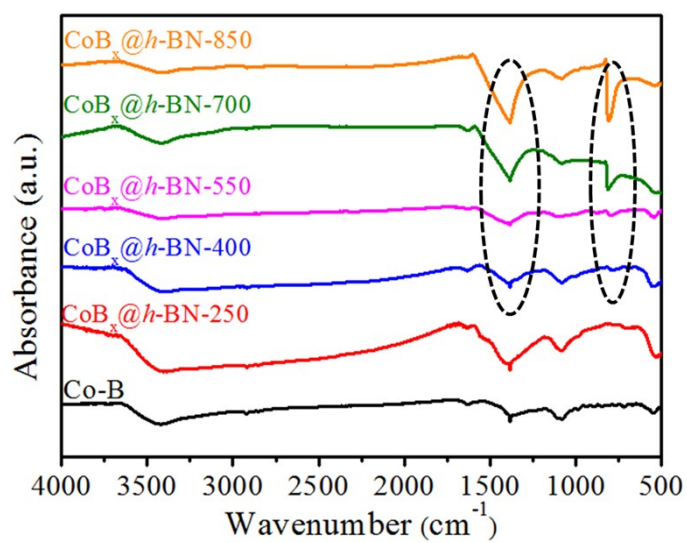


Figure S4 FTIR spectra of Co-B and $\text{CoB}_x@h\text{-BN-T}$ samples.

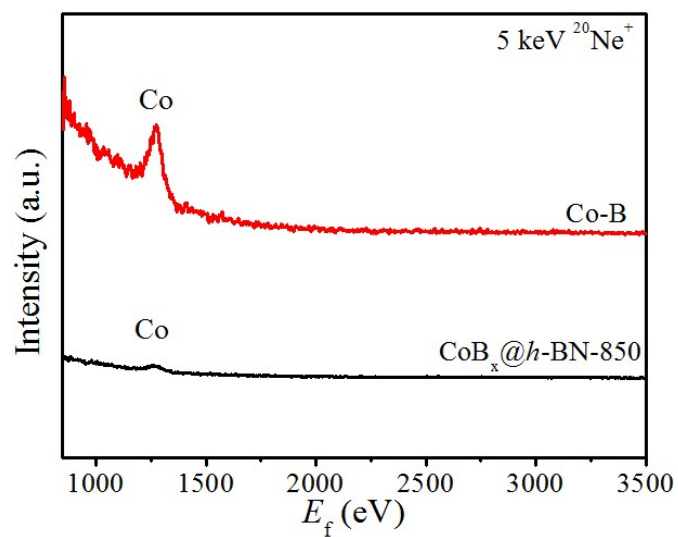


Figure S5 HS-LEIS spectra of Co-B and $\text{CoB}_x@h\text{-BN-850}$ samples. $^{20}\text{Ne}^+$ ions with a kinetic energy of 5 keV were applied.

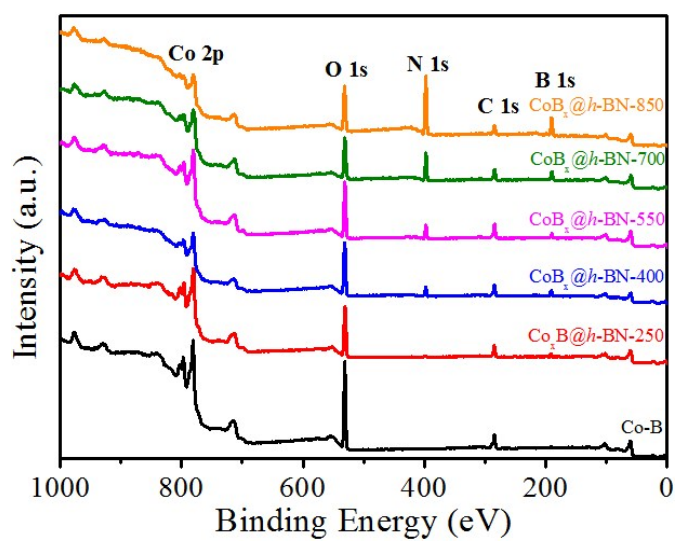


Figure S6 XPS survey spectra of Co-B and $\text{Co}_x@h\text{-BN-T}$ samples.

Table S1 Quantitative analyses of Co-B and Co_x@*h*-BN-T catalysts from XPS measurements.

Sample	B%	B-O	B-N	B-Co	N%	Co%	O%
Co-B	6.57	83.37%	0	17.63%	0.23	8.97	58.27
CoB_x@<i>h</i>-BN-250	12.96	94.79%	0	5.21%	1.22	18.64	45.97
CoB_x@<i>h</i>-BN-400	22.47	60.44%	39.56%	0	9.09	9.61	39.21
CoB_x@<i>h</i>-BN-550	18.31	30.26%	69.74%	0	11.13	7.45	19.60
CoB_x@<i>h</i>-BN-700	28.73	18.88%	81.12%	0	21.73	4.84	25.24
CoB_x@<i>h</i>-BN-850	38.50	0	100%	0	31.34	2.20	18.08

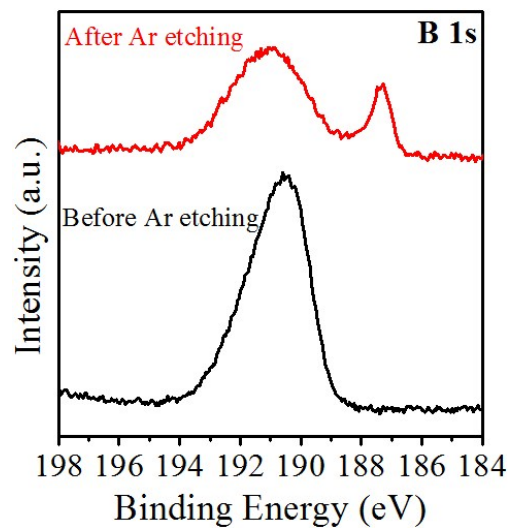


Figure S7 XPS B1s spectra of the CoB_x@h-BN-400 sample before and after Ar⁺ etching treatments.

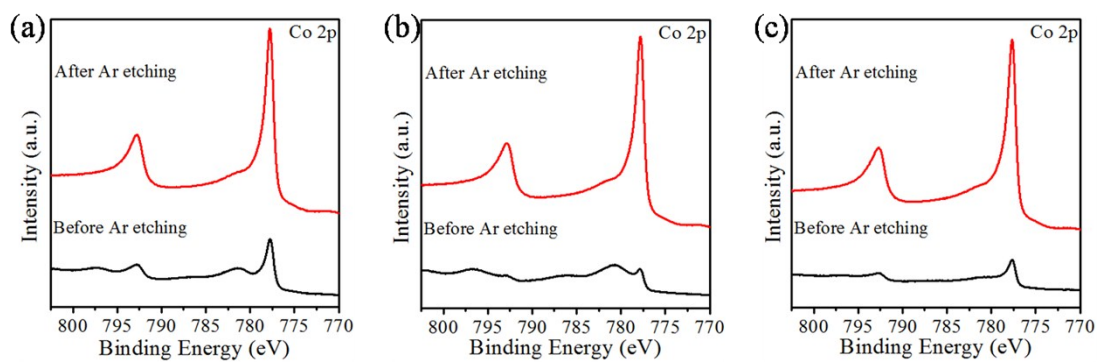


Figure S8 XPS Co 2p spectra of (a) Co-B, (b) CoB_x@h-BN-400, and (c) CoB_x@h-BN-850 samples before and after Ar⁺ etching treatments.

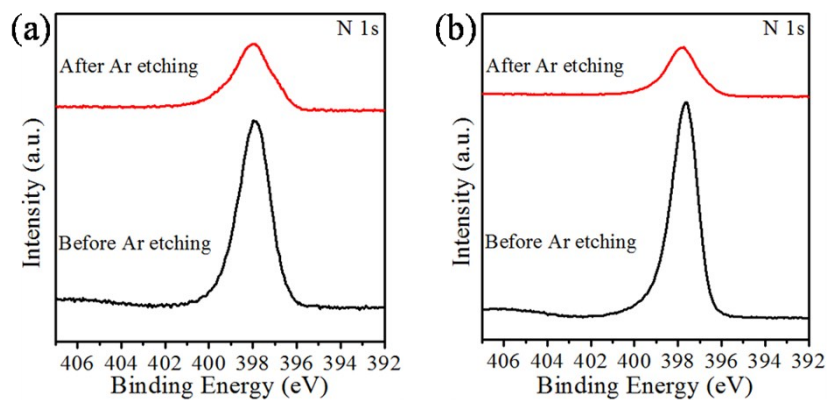


Figure S9 XPS N 1s spectra of (a) $\text{CoB}_x@h\text{-BN-400}$ and (b) $\text{CoB}_x@h\text{-BN-850}$ samples before and after Ar^+ etching treatments.

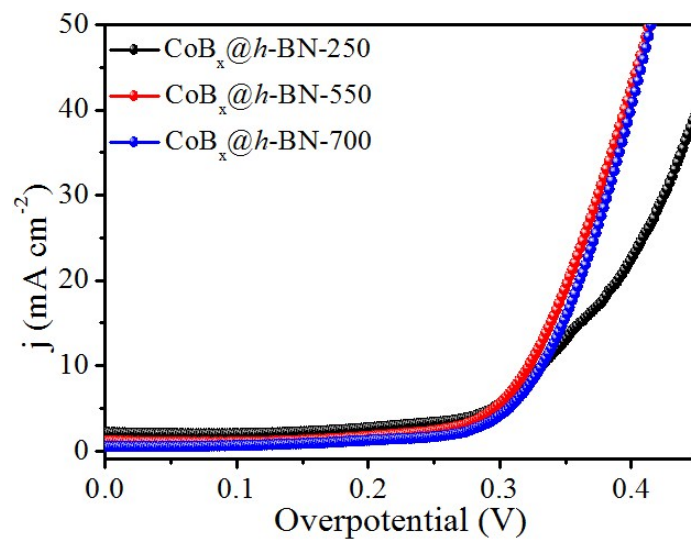


Figure S10 OER polarization curves for $\text{CoB}_x@h\text{-BN-250}$, $\text{CoB}_x@h\text{-BN-550}$, and $\text{CoB}_x@h\text{-BN-700}$ catalysts.

Table S2 Summary for the properties of recent reported OER catalysts.

Catalyst	Electrolyte	Overpotential @10 mA cm ⁻² / mV	Tafel slope / mV dec ⁻¹	Reference
CoBx@h-BN-400	1 M KOH	290	81.9	This work
CoO _x -ZIF	1 M KOH	318	70	1
CoSe ₂	1 M KOH	330	79	2
CoP hollow polyhedra	1 M KOH	400	57	3
CoO _x @CN	1 M KOH	370	N.A.	4
NiCoP/C	1 M KOH	330	96	5
Fe-Co-2.3Ni-B	1 M KOH	274	38	6
Co ₂ B	1 M KOH	287	50.7	7
Ni-B _i @NB	1 M KOH	302	52	8
FeB ₂	1 M KOH	296	52.4	9
Co ₂ B-500/NG	0.1 M KOH	380	45	10

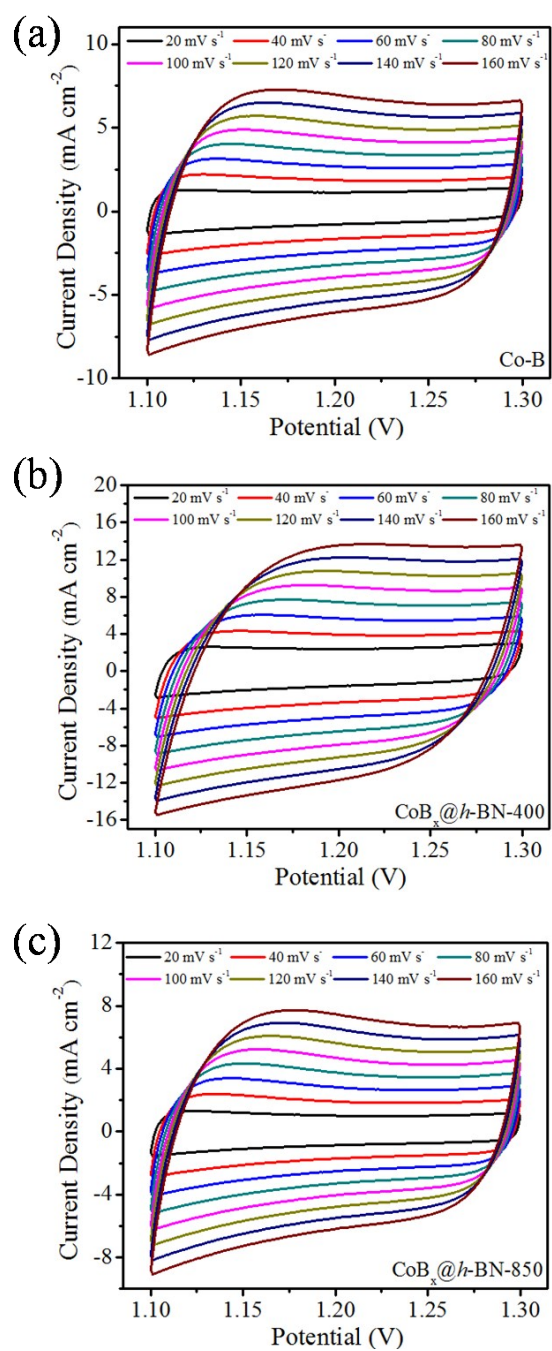


Figure S11 Cyclic voltammogram in the double layer region at scan rate of 20, 40, 60, 80, 100, 120, 140, 160 mV/s of (a) Co-B, (b) CoB_x@h-BN-400, and (c) CoB_x@h-BN-850 catalysts.

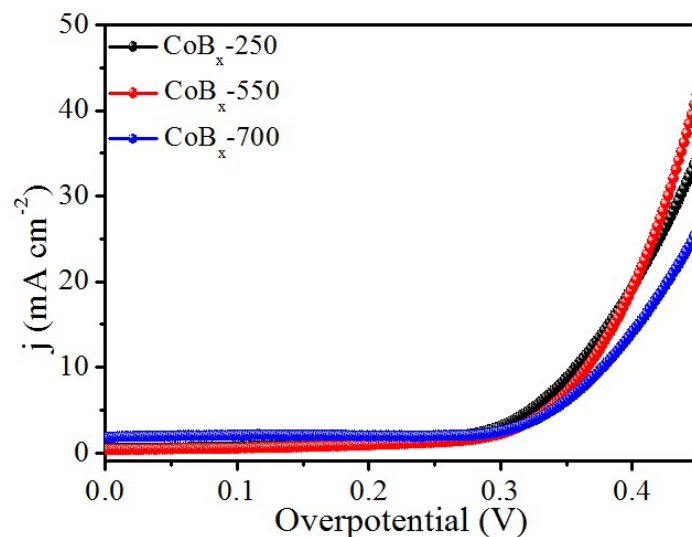


Figure S12 OER polarization curves for CoB_x -250, CoB_x -550, and CoB_x -700 catalysts.

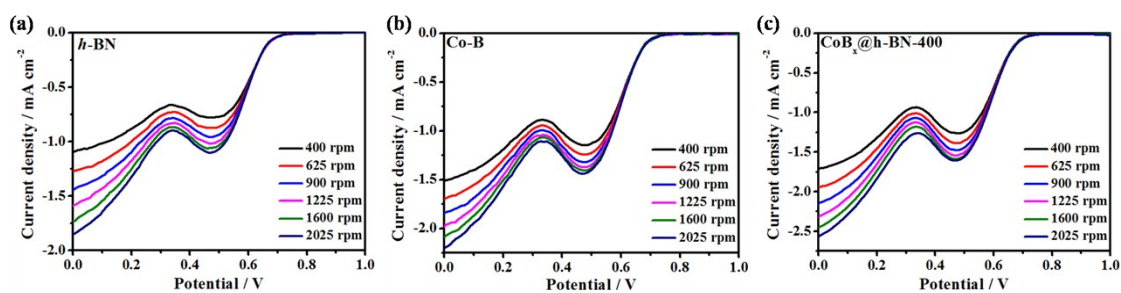


Figure S13 ORR polarization curves at different rotating speeds in 1 M KOH with a sweep rate of 10 mV s^{-1} : (a) *h*-BN, (b) Co-B, (c) CoB_x @*h*-BN-400 catalysts.

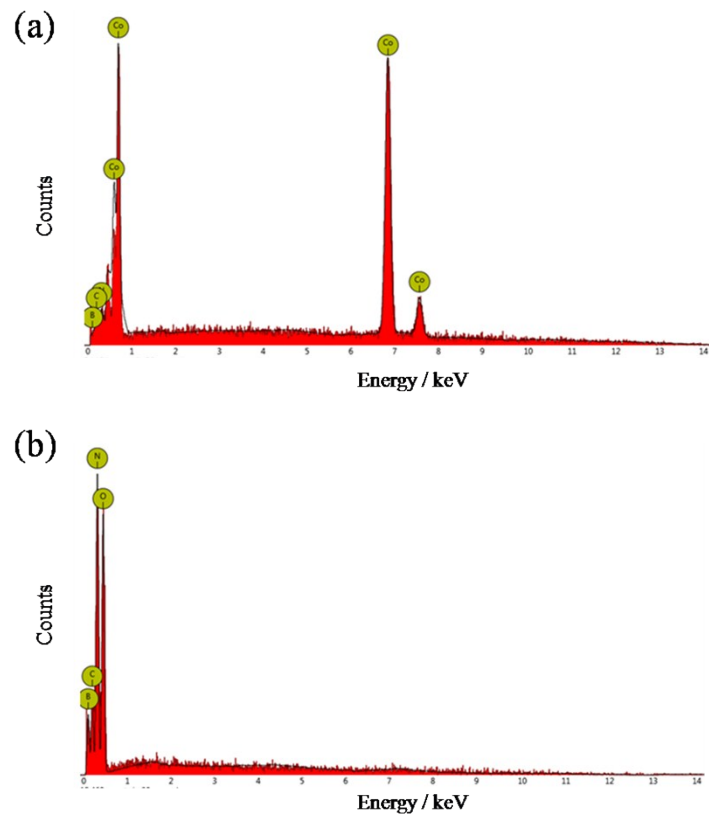


Figure S14 EDS spectra for (a) $\text{CoB}_x@h\text{-BN-850}$ sample, and (b) $h\text{-BN}$ obtained from acid-treated $\text{CoB}_x@h\text{-BN-850}$ sample. The signals of C element come from conducting resin.

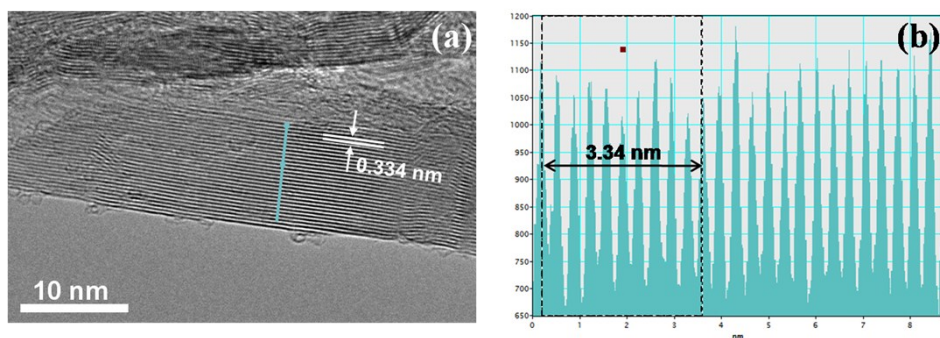


Figure S15 HRTEM image of $h\text{-BN}$ obtained from acid-treated $\text{CoB}_x@h\text{-BN-850}$ sample and the measured layer distances.

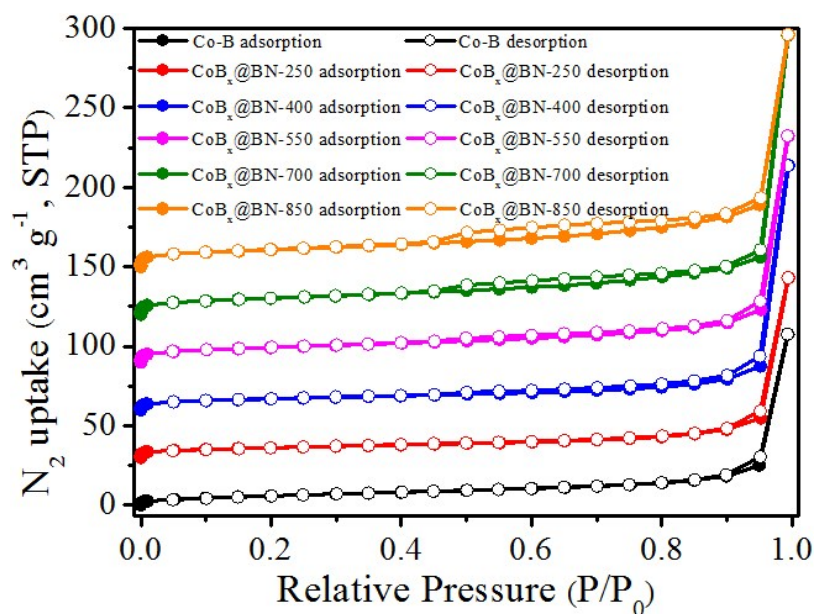


Figure S16 Nitrogen adsorption-desorption isotherms of Co-B and $\text{CoB}_x@h\text{-BN-T}$ catalysts.

Table S3 BET surface area and the elemental composition of B and Co determined by ICP-OES in Co-B and $\text{CoB}_x@h\text{-BN-T}$ catalysts.

Sample	BET ($\text{m}^2 \text{g}^{-1}$)	B%	Co%	Atomic Ratio (B:Co)
Co-B	22.40	2.93	87.19	1:5.5
$\text{CoB}_x@h\text{-BN-250}$	22.00	2.98	89.20	1:5.5
$\text{CoB}_x@h\text{-BN-400}$	24.38	2.89	90.09	1:5.7
$\text{CoB}_x@h\text{-BN-550}$	32.80	3.02	92.13	1:5.6
$\text{CoB}_x@h\text{-BN-700}$	35.94	3.02	91.38	1:5.6
$\text{CoB}_x@h\text{-BN-850}$	37.79	3.11	96.75	1:5.7

Reference:

1. S. Dou, C. Dong, Z. Hu, Y. Huang, J. Chen, L. Tao, D. Yan, D. Chen, S. Shen, S. Chou and S. Wang, *Adv. Funct. Mater.*, 2017, 1702546.
2. X. Liu, Y. Liu and L. Fan, *J. Mater. Chem. A*, 2017, **5**, 15310.
3. D. Zhou, L. He, W. Zhu, X. Hou, K. Wang, G. Du, C. Zheng, X. Sun, and A. M. Asiri, *J. Mater. Chem. A*, 2016, **4**, 10114-10117.
4. H. Jin, J. Wang, D. Su, Z. Wei, Z. Pang and Y. Wang, *J. Am. Chem. Soc.*, 2017, **137**, 2688.
5. P. He, X. Yu and X. (David) Lou, *Angew. Chem. Int. Ed.*, 2017, **129**, 3955.
6. J. Nsanzimana, Y. Peng, Y. Xu, L. Thia, C. Wang, B. Xia, X. Wang, *Adv. Energy Mater.*, 2017, 1701475.
7. X. Ma, J. Wen, S. Zhang, H. Yuan, K. Li, F. Yan, X. Zhang and Y. Chen, *ACS Sustainable Chem. Eng.*, 2017, **5**, 10266.
8. W-J. Jiang, S. Niu, T. Tang, Q-H Zhang, X-Z Liu, Y. Zhang, Y-Y Chen, J-H Li, L. Gu, L-J. Wan, J-S. Hu, *Angew. Chem. Int. Ed.*, 2017, **56**, 6572.
9. H. Li, P. Wen, Q. Li, C. Dun, J. Xing, C. Lu, S. Adhikari, L. Jiang, D. L. Carroll, S. M. Geyer, *Adv. Energy Mater.*, 2017, **17**, 1700513.
10. J. Masa, P. Weide, D. Peeters, I. Sinev, W. Xia, Z. Sun, C. Somsen, M. Muhler and W. Schuhmann, *Adv. Energy Mater.*, 2016, **6**, 1502313.